Antonini, E., & Brunori, M. (1971) *Hemoglobin and Myoglobin in Their Reactions with Ligands*, North-Holland, Amsterdam.
Baroin, A., Bienvenue, A., & Devaux, P. F. (1979) *Biochemistry 18*, 1151–1155.
Beth, A. H., Wilder, R., Wilkerson, L. S., Perkins, R. C., Merriwether, B. P., Dalton, L. R., Park, C. R., & Park, J. H. (1979) *J. Chem. Phys. 71*, 2074–2082.
Davoust, J., Bienvenue, A., Fellman, P., & Devaux, P. F. (1980) *Biochim. Biophys. Acta 596*, 28–42.
deJager, P. A., & Hemminga, M. A. (1978) *J. Magn. Reson. 31*, 491–496.
Delmelle, M., Butler, K. W., & Smith, I. C. P. (1980) *Biochemistry 19*, 698–704.
Fung, L. W.-M., Soo Hoo, M. J., & Meena, W. A. (1979) *FEBS Lett. 105*, 379–383.
Gaffney, B. J. (1979) *J. Phys. Chem. 83*, 3345–3349.
Hyde, J. S. (1978) *Methods Enzymol. 49*, 480–511.
Hyde, J. S., & Thomas, D. D. (1973) *Ann. N.Y. Acad. Sci. 222*, 680–692.
Hyde, J. S., & Dalton, L. R. (1979) in *Spin Labeling; Theory and Applications* (Berliner, L. J., Ed.) Vol. 2, pp 1–70, Academic Press, New York.
Hyde, J. S., & Thomas, D. D. (1980) *Annu. Rev. Phys. Chem. 31*, 293–317.
Johnson, M. E. (1978) *Biochemistry 17*, 1223–1228.
Jones, C. R., Johnson, C. S., & Penniston, J. T. (1978) *Biopolymers 17*, 1581–1593.
Kusumi, A., Ohnishi, S., Ito, T., & Yoshizawa, T. (1978) *Biochim. Biophys. Acta 507*, 539–543.
Lemaigre-Dubreuil, Y., Henry, Y., & Cassoly, R. (1980) *FEBS Lett. 113*, 231–234.
Marsh, D. (1980) *Biochemistry 19*, 1632–1637.
Robinson, B. H., & Dalton, L. R. (1979) *Chem. Phys. 36*, 207–237.
Robinson, B. H., & Dalton, L. R. (1980) *J. Chem. Phys. 72*, 1312–1324.
Swift, L. L., Atkinson, J. B., Perkins, R. C., Dalton, L. R., & LeQuire, V. S. (1980) *J. Membr. Biol. 52*, 165–172.
Thomas, D. D., Dalton, L. R., & Hyde, J. S. (1976) *J. Chem. Phys. 65*, 3006–3024.
Thomas, D. D., Seidel, J. L., & Gergely, J. (1979) *J. Mol. Biol. 132*, 257–273.
Trommer, W. E., & Glöggler, K. (1979) *Biochim. Biophys. Acta 571*, 186–194.

# Laser Chemically Induced Dynamic Nuclear Polarization Study of the Reaction between Photoexcited Flavins and Tryptophan Derivatives at 360 MHz†

Elizabeth F. McCord, Rodney R. Bucks, and Steven G. Boxer*

ABSTRACT: Chemically induced dynamic nuclear polarization (CIDNP) is generated when tryptophan (Trp), its derivatives, or Trp-containing peptides react with photoexcited flavins in a 360-MHz NMR spectrometer. In contrast to tyrosine (Tyr), we find that the nuclear polarization of Trp originates in an electron-transfer reaction. By use of a series of Trp derivatives, the unpaired spin-density distribution of the Trp radical cation and the ground-state NMR spectrum of Trp are analyzed in detail. The signs and the relative magnitudes of the proton isotropic hyperfine coupling constants for each position around the indole ring in the radical cation deduced from these measurements are the following: position $3 \gg 2 \sim 4 \sim 6 > 1 \gg 5 > 7$, with positions 1, 2, 3, 4, and 6 positive, 5 negative, and 7 essentially zero. This result is inconsistent with most available calculations of the unpaired spin-density distribution but is compatible with the pattern of electrophilic aromatic substitution. The origin of this discrepancy is discussed in detail. Possible mechanistic complications in the reaction leading to CIDNP are discussed. The laser CIDNP spectra of the Trp-rich peptides gramicidins A and B are presented as examples of the resolution enhancement obtained with this technique.

The photophysics and photochemistry of both tryptophan (Trp)[1] and flavins have been studied extensively and exploited to probe their environment and reactivity in a large number of proteins. Trp is a very useful reporter because it can be selectively excited, and its fluorescence emission provides a probe of local conformational flexibility (Munro et al., 1979) or dielectric properties in the protein (Donovan, 1969). It is ideally suited for structural studies in proteins using resonant energy transfer to or from other residues or prosthetic groups (Stryer & Haugland, 1967; Yguerabide et al., 1970). Recently, the properties of the Trp triplet state have been used

† From the Department of Chemistry, Stanford University, Stanford, California 94305. *Received October 30, 1980.* This research was supported by the Research Corporation and National Institutes of Health Grant GM 27738. The 360-MHz NMR spectra were obtained at the Stanford Magnetic Resonance Laboratory supported by National Science Foundation and National Institutes of Health Grants GR 23633 and RR 00711, respectively. E.F.M. is the recipient of a National Science Foundation Predoctoral Fellowship, and S.G.B. is an Alfred P. Sloan and Camille and Henry Dreyfus Teacher-Scholar Fellow.

[1] Abbreviations used: CI, configuration interaction; CIDNP, chemically induced dynamic nuclear polarization; COT, cyclooctatetraene; $Me_2SO$, dimethyl sulfoxide; ESR, electron spin resonance; His, histidine; HMO, Huckel molecular orbital; HOMO, highest occupied molecular orbital; INDO, intermediate neglect of differential overlap; LCAO, linear combination of atomic orbitals; LUMO, lowest unoccupied molecular orbital; MO, molecular orbital; NMR, nuclear magnetic resonance; Phe, phenylalanine; SCE, standard calomel electrode; SCF, self-consistent field; TBAP, tetra-*n*-butylammonium perchlorate; $Me_4Si$, tetramethylsilane; Trp, tryptophan; Tyr, tyrosine.

0006-2960/81/0420-2880$01.25/0 

Scheme I: Hydrogen Abstraction

$$F \xrightarrow{h\nu} {}^1F \longrightarrow {}^3F \quad (1)$$

$${}^3F + AH \longrightarrow {}^3\overline{FH\cdot\ A\cdot} \quad (2)$$

$${}^3\overline{FH\cdot\ A\cdot} \longrightarrow {}^*F + {}^*AH \quad (3)$$

$${}^3\overline{FH\cdot\ A\cdot} \longrightarrow FH\cdot + A\cdot \quad (4)$$

$$FH\cdot + A\cdot \longrightarrow {}^*F + {}^*AH \quad (5)$$

to examine the local environment of this residue and its proximity to paramagnetic transition metals in proteins (Maki & Zuchlich, 1975; Ross et al., 1980).

Photoionization to form the Trp cation radical is an important pathway for deactivation of the Trp excited singlet state (Fleming et al., 1978); however, very little ESR data have been obtained for this important radical due to its instability in fluid solution. A number of photoexcited dye molecules sensitize the oxidation of Trp or directly attack it (Saito et al., 1977; Heelis et al., 1978). In particular, the reactions between photoexcited flavins and Trp have been extensively investigated because the fluorescence quantum yield of flavins in a number of flavoproteins is unusually low due to quenching by Trp residues near the active site (McCormick, 1977).

Kaptein and co-workers (Kaptein et al., 1978a,b; Kaptein, 1978) have recently shown that radical pairs must be involved in the reaction between photoexcited flavins and Trp in solution because chemically induced dynamic nuclear polarization (CIDNP) is observed when the reaction is monitored in an NMR spectrometer. CIDNP is observed as greatly enhanced absorption or emission in the NMR signals of the diamagnetic products of reactions in which radical pairs are intermediates (Lepley & Closs, 1973; Muus et al., 1977). This deviation in magnitude from the Boltzmann population difference is commonly denoted spin polarization. Because photoexcited flavins can form radical pairs with accessible Trp, His, and Tyr residues, the NMR signals associated with these residues are substantially enhanced and readily detected in the presence of the unaffected background protein NMR spectrum by difference methods. We are interested in applying this method to determine the location and reactivity of Trp in a number of small peptides, such as the gramicidins and integral membrane proteins. While pursuing this goal, it became apparent that the mechanism of the photochemical reaction between Trp and flavins is not entirely clear. Furthermore, the polarization pattern suggested proton hyperfine coupling constants which were not intuitively expected, so we have undertaken a more detailed investigation of this reaction.

The mechanism which leads to spin polarization for Tyr is shown in Scheme I. The flavin (F) is selectively excited with 488-nm light from an argon ion laser and intersystem crosses to the triplet state (step 1), which abstracts a hydrogen atom from the heteroatom of the amino acid side chain (AH) to form a radical pair (step 2, the horizontal bar denotes a spin-correlated radical pair). The reaction is reversible, and spin polarization (indicated in the diamagnetic products with an *) is preferentially detected from the geminate recombination pathway (step 3), as the opposite spin polarization in the identical products of the escape pathway (step 5) is attenuated by relaxation during the lifetime of the escaping radicals in step 4 (Lamola et al., 1975; Boxer, 1976; Kaptein et al., 1978b).

For Trp, the electron-transfer pathway shown in Scheme II may also be operative, and there is some precedent for this mechanism in the literature on flavin and Trp photochemistry (Ballard et al., 1976). An electron-transfer reaction may be

Scheme II: Electron Transfer

$$F \xrightarrow{h\nu} {}^1F \longrightarrow {}^3F \quad (1)$$

$${}^3F + AH \longrightarrow {}^3\overline{F^-\cdot\ AH^+\cdot} \quad (2)$$

$${}^3\overline{F^-\cdot\ AH^+\cdot} \longrightarrow {}^*F + {}^*AH \quad (3)$$

$${}^3\overline{F^-\cdot\ AH^+\cdot} \longrightarrow F^-\cdot + AH^+\cdot \quad (4)$$

$$F^-\cdot + AH^+\cdot \longrightarrow {}^*F + {}^*AH \quad (5)$$

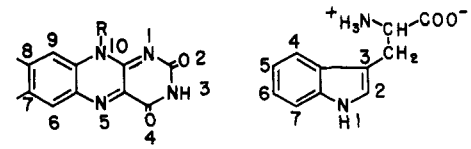

FIGURE 1: Structures and numbering systems for flavins and Trp. Riboflavin has R = D-ribo-2,3,4,5-tetrahydroxypentyl; lumiflavin has R = methyl.

less dependent on direct molecular collision than hydrogen abstraction; thus, CIDNP for Trp may not be a direct probe of accessibility, as is probable for His or Tyr, but may probe the more subtle and equally interesting nature of electron-transfer pathways in proteins. In this paper, we analyze the CIDNP from the reaction of Trp with photoexcited riboflavin or lumiflavin in detail and find that electron transfer plays a significant role. The CIDNP data also provide direct information on the spin-density distribution in this important amino acid radical.

## Experimental Procedures

All compounds were obtained commercially with the exception of 1,3-dimethylindole, which is synthesized from 3-methylindole (Potts & Saxton, 1973), DL-2-methyltryptophan, which is synthesized from 2-methylindole (Rydon, 1948), and the methyl esters, which are prepared from the corresponding acids by using methanolic hydrochloric acid. The indoles and carbazoles are purified by sublimation or vacuum distillation, and riboflavin is recrystallized from water. The purified gramicidins are a generous gift from Professor Stryer. The pH values of deuterated buffers are measured with a glass electrode and are not corrected for the isotope effect. Solutions are not degassed, except for those used in the $T_1$ measurements (five freeze–pump–thaw cycles at $10^{-4}$ torr). The structures and numbering systems for Trp and the flavins are shown in Figure 1.

A proton probe for the 360-MHz NMR spectrometer at the Stanford Magnetic Resonance Laboratory has been constructed to permit laser irradiation of the sample during the NMR experiment. The laser source is a continuous argon ion laser operated at 488 nm (1.4 W). The laser beam is directed into the NMR sample tube from the side, using a 45° mirror, as illustrated in Figure 2. This arrangement maximizes the irradiated volume in the region of the receiver coil and does not perturb field homogeneity. The computer controls both the duration of irradiation, using an interfaced shutter, and the radio frequency (rf) pulsing. Typically, the sample is irradiated for 0.5 s, followed by a 1-ms delay, the rf pulse, and data acquisition. This technique minimizes line broadening from triplet or electron exchange (Boxer & Closs, 1975; Boxer, 1976; Kaptein et al., 1978b). Light minus dark difference spectra are obtained in subsequent processing.

Cyclic voltammograms are recorded at 23 °C by using a three-compartment three-electrode cell with platinum wire working and counter electrodes and a 0.1 M lithium chloride salt bridge to the SCE reference electrode. Tetra-*n*-butyl-

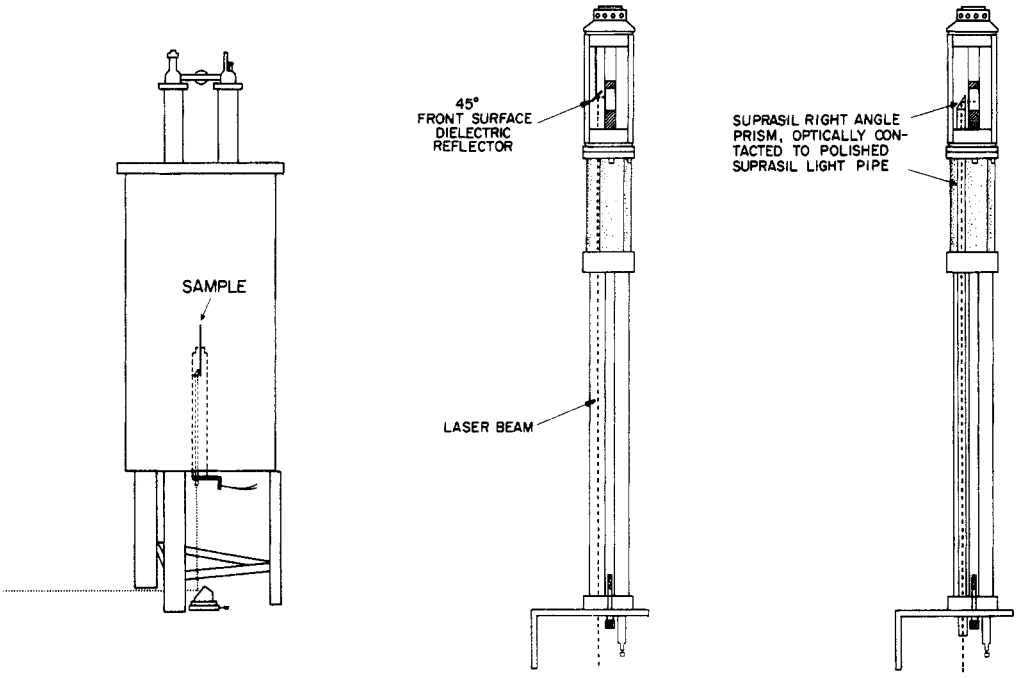


FIGURE 2: $^1$H NMR (360 MHz) setup and probe used for the experiments reported in this paper. The mirror is a microscope cover slip coated with a dielectric reflector for >99.9% reflection of the argon ion blue-green lines. Alternately, a quartz light pipe with optically contacted prism can be used for excitation at any wavelength in the range 200–1200 nm.

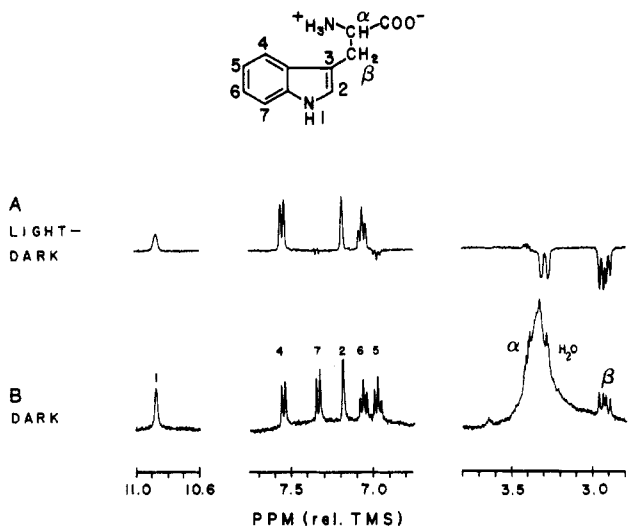


FIGURE 3: $^1$H NMR spectra (360 MHz) of L-Trp (10 mM) and riboflavin (1 mM) in $Me_2SO$-$d_6$. Single dark and light pulses were alternately acquired and averaged (eight pulses total of each). The broad peak under the aromatic protons is $-NH_3^+$, and the broad peak around 3.3–3.4 ppm is $H_2O$ in the solvent. Tryptophan methyl ester, *N*-acetyltryptophan, and *N*-acetyltryptophan methyl ester exhibit identical polarization patterns.

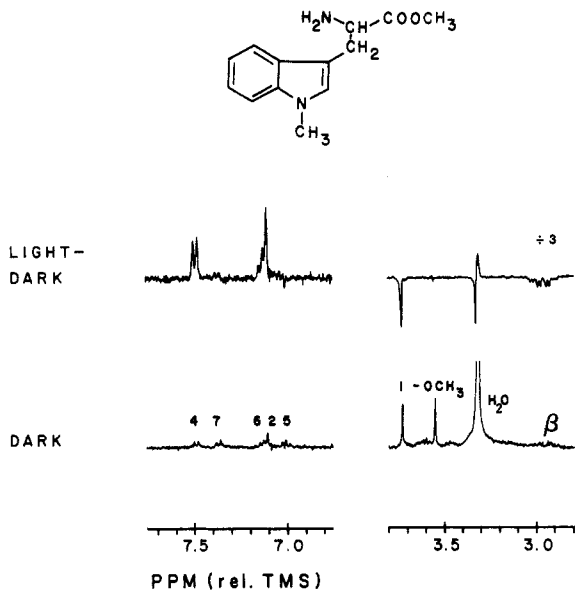


FIGURE 4: $^1$H NMR spectra (360 MHz) of DL-1-methyltryptophan methyl ester (2.3 mM) and riboflavin (1 mM) in $Me_2SO$-$d_6$. Experimental conditions identical with those in Figure 3.

ammonium perchlorate is recrystallized 4 times from ethyl acetate and dried in vacuo at 100 °C for 24 h. Acetonitrile is purified by using the method recommended by Sawyer & Roberts (1974). The samples are 0.5–3.0 mM, and the electrolyte is 0.2 M in degassed acetonitrile. The peak potentials depend on scan rate; the values reported below are recorded at 100 mV/s.

## Results and Discussion

*Mechanism.* A series of Trp derivatives was studied in various solvents. Figures 3 and 4 show light minus dark difference spectra of L-tryptophan and DL-1-methyltryptophan methyl ester. Both molecules exhibit spin polarization with a similar pattern, even though the latter has no hydrogen to abstract from the aromatic nitrogen. This strongly suggests that the polarization is generated in a reversible electron-transfer reaction (Scheme II). Cyclooctatetraene (COT), a well-known triplet quencher, strongly attenuates the polarization. COT has been shown to quench the triplet state of dyes such as Rhodamine 6G (Yamashita & Kashiwagi, 1974), whose triplet energy of 43.7 kcal is lower than 50 kcal, the triplet energy of riboflavin (Chambers & Kearns, 1969; Sandros, 1964). We also find that COT has no affect on the fluorescence quantum yield of riboflavin. It is conceivable that other radical intermediates involving rearrangement or attack by the solvent or impurities may contribute to the polarization. We find that the polarization pattern is independent of solvent ($Me_2SO$, water, or methanol), the presence of oxygen, and ring substituents, and no other spin-polarized species except the flavin are detected. Since polarization is only detected in the

starting material by geminate recombination, the pattern of Trp polarization almost certainly reflects the radical cation intermediate (vide infra). Side reactions of the riboflavin do occur, leading to bleaching of the dye. For this reason, the sample is mixed between irradiations.[2]

It is reasonable to assume that the largest spin polarization for aromatic protons is associated with positive spin density in the precursor radical at the adjacent carbon atom. By application of the well-known rules governing the sign of nuclear polarization for a triplet reaction and a geminate recombination pathway (Closs & Trifunac, 1970; Kaptein, 1971), the positive polarization of these protons implies that the $g$ factor for the Trp radical cation must be less than that of the flavin radical anion ($g$ = 2.0032 for the neutral and 2.0034 for the anionic lumiflavin radical; Eriksson & Ehrenberg, 1964).

Confirmation of this mechanism for Trp itself is obtained from an analysis of the positive polarization observed for the aromatic NH proton in Figure 3. If this proton were abstracted by the flavin, it would reside on the flavin radical at nitrogen atom 5 (Müller et al., 1970). This radical has been studied by Eriksson & Ehrenberg (1964), and a detailed analysis of the ESR spectrum demonstrates that the spin density at this nitrogen is large and positive. Thus, we would expect negative spin density at the hydrogen during its residence on the flavin radical and would predict negative polarization, contrary to what is observed in Figure 3. We have also observed the Trp NH proton in enhanced absorption during irradiation in ordinary water by using a Redfield 214 pulse sequence (Redfield & Kunz, 1979; Redfield et al., 1975). By comparison, we have observed weak enhanced absorption for the phenolic proton in *N*-acetyltyrosine amide in $Me_2SO$-$d_6$, while the largest polarization is associated with the ortho protons which are strongly polarized in emission; tyrosine methyl ether shows no polarization.

*Energetics.* In contrast to 1-methyltryptophan methyl ester, we were surprised to find that 1-methylindole and 1,3-dimethylindole show only very weak spin polarization under identical conditions. All the other methylindoles, as well as indole itself (see Figure 7A), are comparable with Trp. This led us to consider the possibility that an electron-transfer reaction might be energetically unfavorable for these derivatives. We can estimate the free-energy change for an electron-transfer reaction from the following expression (Knibbe et al., 1968):

$$\Delta G = E(\mathrm{D}/\mathrm{D}^{+}\cdot) - E(\mathrm{A}^{-}\cdot/\mathrm{A}) - E(^3\mathrm{A}) - e_0^2/\epsilon a$$

where $E(\mathrm{D}/\mathrm{D}^{+}\cdot)$ is the one-electron oxidation potential of the donor, $E(\mathrm{A}^{-}\cdot/\mathrm{A})$ is the one-electron reduction potential of the acceptor, $E(^3\mathrm{A})$ is the energy of the lowest triplet state of the acceptor, and $e_0^2/\epsilon a$ accounts for the coulombic interaction of an ion pair in the encounter complex with charge $e_0$, bulk dielectric constant $\epsilon$, and distance of separation $a$. For $a$ = 7 Å (Knibbe et al., 1968), the latter term is 1.05 kcal in $Me_2SO$; the riboflavin triplet energy is 50 kcal (Chambers & Kearns, 1969); the one-electron reduction potential of riboflavin in $Me_2SO$ is approximately –0.75 V vs. SCE (Tatwawadi et al., 1968). From this analysis, we estimate that an electron-transfer reaction would be thermodynamically unfavorable if the oxidation potential of Trp or its derivatives were greater than approximately 1.4 V vs. SCE.

The oxidation potentials of a few indole derivatives have been reported in the literature (Yoshida, 1979), and we have investigated a more extensive series of indoles by cyclic voltammetry. Unfortunately, it did not prove possible to observe reversible waves regardless of the scan rate, and it appears that the anodic electrochemistry of these compounds involves electrochemical oxidation, a following chemical reaction, and subsequent electrochemical oxidation of the reaction product [an ECE mechanism, see Nicholson & Shain (1965)]. Exactly this behavior has been reported for the electrochemical oxidation of the carbazoles by Ambrose et al. (1975). With the indoles, no cathodic peaks are observed (except in the case of 1,3-dimethylindole at very high scan rates), and severe electrode filming in most cases suggests that rapid polymerization of the oxidation product(s) is occurring. The anodic peak potentials (volts vs. SCE ± 0.02 V) measured in acetonitrile for substituted indoles are the following: 1-methyl, 1.16; 3-methyl, 1.01; 1,3-dimethyl, 0.97; 4-methyl, 1.11; 7-methyl, 1.11; 2-methyl, 1.03; indole itself, 1.20. These peak potentials were also measured in $Me_2SO$ with TBAP, though an apparent IR drop due to solvent and/or electrolyte oxidation introduced large uncertainties into these measurements (small variations in the electrode position shifted the peak potential). This is not surprising, considering that the anodic voltage limit with this electrolyte in $Me_2SO$ is generally considered to be 0.7 V vs. SCE (Sawyer & Roberts, 1974; Koch & Purdy, 1972). The general ordering of the oxidation peak potentials is identical with both solvents; actual numerical values are somewhat higher in $Me_2SO$. The relative peak potentials listed above do not correlate with the observed CIDNP intensities; however, the measured peak potentials may be shifted substantially from the true thermodynamic potentials by irreversibility or quasi-irreversibility of the electrochemical oxidation, as well as by the varying rates of the irreversible following chemical reaction. Nonetheless, we note that the potentials of all these derivatives are below 1.4 V vs. SCE, so it is unlikely that the differences in CIDNP intensities among these compounds are related primarily to reaction energetics.

*Concentration Dependence.* In the course of these experiments, we noted that 1-methyltryptophan also gives weaker polarization than Trp under comparable conditions and that the absolute magnitude of the polarization depends strongly on concentration. We therefore undertook a detailed comparative study of the concentration dependence of the nuclear polarization from tryptophan methyl ester·HCl and 1-methyltryptophan methyl ester·HCl (the methyl esters are used because they are more soluble in $Me_2SO$-$d_6$). The enhancement factor (the integral of the light minus dark signal divided by the integral of the dark signal) decreases rapidly with increasing Trp derivative concentration in the range 0.5 to 50 mM. This decrease is much more dramatic for 1-methyltryptophan than for Trp: for example, 50 mM 1-methyltryptophan shows virtually no polarization, whereas the two compounds show equal polarization at 0.5 mM.

A probable explanation for these observations is shown in the following modifications of step 4 in Scheme II, where

[2] This problem has not been addressed before and applies equally to experiments involving His, Tyr, and these residues in proteins. If the sample is not mixed adequately between light pulses, the CIDNP intensity is considerably weaker on successive light pulses, and subsequent signal averaging is useless. Flavins undergo a number of photochemical reactions independent of their reaction with Trp derivatives. These involve anion–cation formation, reactions with solvent, and a variety of intra- and intermolecular reactions, all of which bleach the dye (Penzer & Radda, 1967; Moore & Baylor, 1969). Sample mixing refreshes the detected volume of the sample with unreacted flavin. Shaking also reintroduces oxygen (depleted during the photoreactions), which can reoxidize any fully reduced flavin that may have been formed in the sample by disproportionation of neutral flavin radicals. We find that for proteins, even in the millimolar concentration range, a single pulse, light minus dark, is sufficient to provide an adequate signal-to-noise ratio.

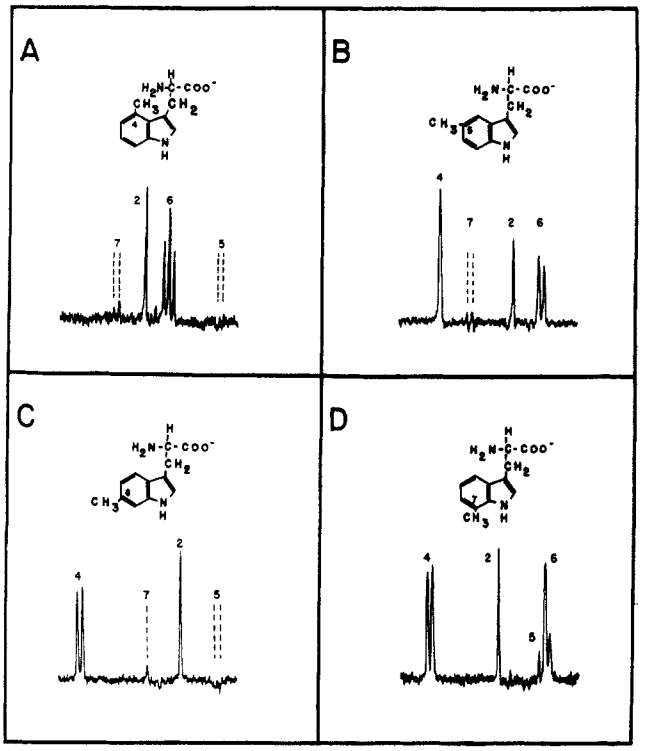


FIGURE 5: $^1$H NMR (360 MHz) light minus dark difference spectra for methyl-substituted DL-tryptophans as illustrated. All samples were 2.5 mM in the Trp derivative, 0.2 mM lumiflavin (pH 10 borate buffer). Dotted lines indicate the positions and multiplicities of resonances which are *not* spin polarized and hence absent in the light minus dark spectra. Each plot covers 0.75 ppm and is the average of eight pulses.

primes denote identical molecules which are not part of the original spin-correlated pair, and S is a proton acceptor. For 1-methyltryptophan (AMe):

$$F^{-}\cdot + AMe^{+}\cdot \xrightarrow[\text{fast}]{AMe'} F^{-}\cdot + {}^{*}AMe + AMe'^{+}\cdot \quad (4a)$$

For Trp (AH):

$$F^{-}\cdot + AH^{+}\cdot \xrightarrow[\text{fast}]{S} F^{-}\cdot + A\cdot + SH^{+} \quad (4b)$$

$$A\cdot + AH' \xrightarrow[\text{slow}]{} {}^{*}AH + A'\cdot \quad (4c)$$

In the case of 1-methyltryptophan at high concentration, the polarization on the escaping radicals can be preserved by biomolecular degenerate electron exchange, converting the radical to a diamagnetic product very rapidly. Therefore, the escape and cage polarization are more effectively cancelled, and little or no CIDNP is detected at high concentrations. For Trp, rapid deprotonation of the cation radical can occur, and the resulting neutral radical must undergo bimolecular hydrogen atom transfer in order to preserve its polarization by this mechanism. Since hydrogen atom exchange is much slower than degenerate electron exchange (Kreilick & Weissman, 1966), the radicals whose nuclear spins carry the escape polarization are preserved longer, and nuclear relaxation in these radicals decreases the escape polarization. This mechanism also provides a simple explanation for the large discrepancy between the polarization magnitudes of the indoles and 1-methylindoles discussed above, which show an analogous concentration dependence. It should be noted that bimolecular exchange is not likely to be significant when the residue is located in a high molecular weight protein, but unusual properties of the local environment may catalyze an intramolecular exchange which could strongly affect the polarization intensity.

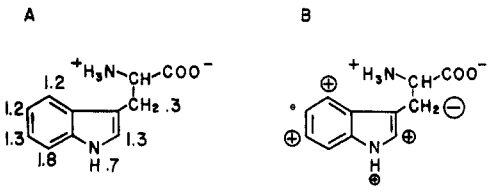


FIGURE 6: (A) Proton spin–lattice relaxation times for Trp in $Me_2SO$-$d_6$ (±0.1 s). $T_1$ values are not noticeably affected by the presence of riboflavin. (B) Schematic representation of the signs and relative magnitudes of Trp ring proton polarizations.

*Assignment of the Trp NMR Spectrum.* Further consideration of the spin-density distribution of the Trp radical cation requires an assignment of the proton aromatic resonances. There has been considerable controversy over this assignment in the literature (Cohen, 1971; Wessels et al., 1973; McDonald & Leigh, 1973), which we can unambiguously resolve by the CIDNP technique. A series of methyl-substituted tryptophans was studied, as shown in Figure 5. The ground-state NMR spectra of the methyltryptophans provide little guidance, as substitution of a methyl group alters the chemical shifts. However, this substitution does not affect the *sign* of the unpaired spin density at the adjacent carbon atom, so the nuclear polarization *pattern* is unperturbed. A self-consistent analysis of these spectra, together with that in Figure 3, leads to the assignment of the proton NMR spectrum shown in Figure 3. As expected, the methyl protons are found in emission when a methyl group is substituted at the 1, 2, 4, or 6 positions, and are not polarized when substituted at the 5 and 7 positions.

*Spin Density in the Trp Radical Cation.* Both the signs and the relative magnitudes of the proton isotropic hyperfine coupling constants for the Trp cation radical can be extracted from the CIDNP intensities. ESR data for the Trp radical have only been reported in the solid state. In these studies, the radical was generated by X or $\gamma$ irradiation, the exact nature of the radical was not firmly established, and nuclear hyperfine coupling was not well resolved (Forbes & Sullivan, 1967; Casteleijn et al., 1964; Pailthorpe & Nicholls, 1971; Flossmann & Westhof, 1978). Apparently, chemical instability has precluded ESR observation of this important radical in liquid solution, but with CIDNP we have the advantage that very short-lived intermediates produce a long-lived change in the NMR signal intensities. In addition to depending on the isotropic proton hyperfine coupling constant, the absolute CIDNP intensity depends on the $g$-factor difference, the light flux, the absorption cross section, the sample geometry, the rate of the reaction, and the nuclear spin–lattice relaxation rate. For this reason, we will consider here the relative hyperfine coupling constants for ring protons, which only require correction for the differences in proton spin–lattice relaxation rates. A further complication arises because the observed nuclear polarization is that difference between cage and escape polarization which results from nuclear relaxation in the escape radicals. We expect that relaxation will be most effective for nuclei with the largest values of the anisotropic hyperfine coupling to the electron, and the magnitude of this interaction will parallel the isotropic coupling constant. As a consequence, protons with a large hyperfine interaction will exhibit enhanced polarization, while those with smaller hyperfines will be diminished. This effect will change neither the sign nor the relative ordering of the coupling constants.

For Trp, aromatic ring proton $T_1$ values in the diamagnetic molecule are comparable, as shown in Figure 6A, and are not a very significant source of CIDNP intensity differences among these protons. Furthermore, the rate of the photochemical

Table I: Molecular Orbital Calculations of Unpaired Electron and Spin-Density Distributions for the Indole and Carbazole Radical Cations

| | indole | | | | | | | | carbazole | | |
|---|---|---|---|---|---|---|---|---|---|---|---|
| atom | *a* | *b* | *c* | *d* | *e* | *f* | *g* | *h* | *i* | *j* | *k* |
| 1 | 0.139 | 0.070 | 0.041 | 0.334 | 0.197 | 0.634 | 0.14 | 0.716 | 0.133 | 0.10 | 0.151 |
| 2 | 0.110 | 0.102 | 0.198 | 0.155 | 0.272 | −0.150 | 0.06 | −0.183 | 0.001 | −0.02 | −0.079 |
| 3 | 0.298 | 0.207 | 0.140 | 0.110 | 0.125 | 0.300 | 0.49 | 0.315 | 0.118 | 0.11 | 0.148 |
| 4 | 0.173 | 0.224 | 0.165 | 0.136 | 0.187 | 0.042 | 0.16 | −0.023 | 0.073 | 0.01 | −0.039 |
| 5 | 0.029 | 0.089 | 0.001 | 0.029 | 0.001 | 0.122 | 0.02 | 0.109 | 0.073 | 0.01 | −0.039 |
| 6 | 0.109 | 0.068 | 0.177 | 0.101 | 0.114 | −0.051 | 0.10 | −0.047 | 0.118 | 0.11 | 0.148 |
| 7 | 0.117 | 0.234 | 0.135 | 0.090 | 0.123 | 0.168 | 0.04 | 0.121 | 0.001 | −0.02 | −0.079 |
| 8 | 0.023 | 0.002 | 0.030 | 0.014 | 0.003 | −0.087 | 0.05 | −0.092 | 0.133 | 0.10 | 0.151 |
| 9 | 0.003 | 0.002 | 0.113 | 0.021 | −0.021 | 0.023 | −0.04 | 0.090 | 0.203 | 0.46 | 0.640 |

[a] Fukui et al. (1954); LCAO-MO. [b] Momicchioli & Rastelli (1967); semiempirical SCF-MO with limited CI. [c] Dewar & Trinajstic (1971); semiempirical SCF-MO. [d] Yoshida (1979); $\omega$ technique. [e] Baudet et al. (1962); SCF-MO with separate calculation of the orbitals of spin $\alpha$ and $\beta$. [g,j] Evleth et al. (1973); open-shell UHF technique with quartet annihilation. [i] Ambrose et al. (1975); HMO. [f,h,k] This work; INDO calculations (Pople & Beveridge, 1970). The indole geometry was taken from the X-ray data of Hanson (1964) for 3-methylindole; the carbazole geometry was taken from the X-ray data of Kurahashi et al. (1969); standard C–H and N–H bond lengths were used (Pople & Beveridge, 1970). Columns *a*, *b*, *c*, *d*, and *i* are the squared coefficients of the ground-state HOMO; columns *e*, *f*, and *k* are calculated distributions of the $\pi$ spin density on the nitrogen or carbon atoms in the radical cations. Columns *g*, *h*, and *j* are the calculated distributions of the $\pi$ spin density on the nitrogen and carbon atoms in the neutral radicals, formed by deprotonation at the nitrogen.

reaction is much faster than these $T_1$ values, and the time of irradiation and detection are shorter; thus, the ratios of the polarizations provide a reasonable estimate for the relative nuclear hyperfine coupling constants in the cation radical. The additional possibility that cross-relaxation or scaler coupling (Closs & Czeropski, 1977, 1978) is responsible for the sign or magnitude of the polarization was checked by selective rf irradiation of each ring position during photoexcitation and the following delay. This has no effect on the CIDNP intensities of the nonirradiated resonances. Indole and a number of substituted indoles have been examined, and all show the identical polarization pattern for protons in the six-membered ring. In addition, the proton at position 3 is very strongly positively polarized (its enhancement is about 5 times greater than the other polarized protons, as seen for indole in Figure 7A), which is consistent with the strong emission observed for the $\beta$-methylene protons of Trp (Figure 3A).

Positive spin density is delocalized throughout both rings onto positions 1, 2, 3, 4, and 6; there is essentially no spin density at positions 5 and 7.[3] These results are illustrated schematically in Figure 6B and should be compared with the results of a number of published calculations of the unpaired electron and spin-density distributions which are listed in Table I (Fukui et al., 1954; Baudet et al., 1962; Momicchioli & Rastelli, 1967; Dewar & Trinajstic, 1971; Evleth et al., 1973; Yoshida, 1979). We have added INDO calculations of the Trp radical cation and the neutral radical, formed by deprotonation at position 1, to this list (Pople & Beveridge, 1970). There is a great deal of variation among these calculations, and only one, that of Evleth et al. (1973), approximates the CIDNP pattern. The CIDNP pattern is, however, consistent with the reactivity of the indoles to electrophilic aromatic substitution, which follows the trend 3 > 2 > 6 > 4 > 5 > 7 (Sundberg, 1970).

The polarization pattern for Trp is especially striking in view of our results for carbazole (Figure 7B) and other closely related amines. In these cases, the relative CIDNP intensities are in excellent agreement with the calculated unpaired electron density distribution, which is presented for carbazole in Table I (Ambrose et al., 1975; Evleth et al., 1973). The

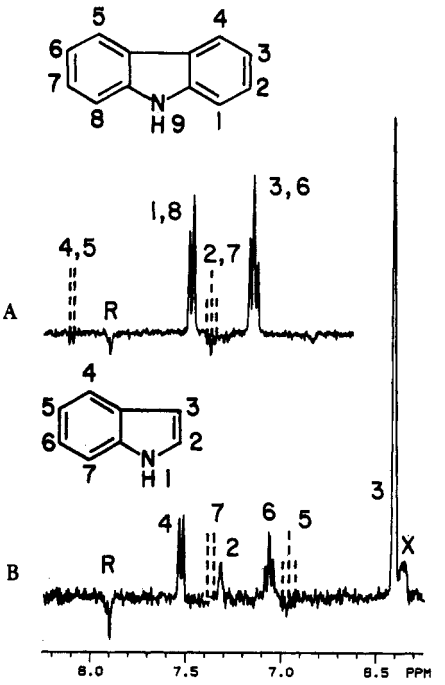


FIGURE 7: Light minus dark difference spectra for (A) 3 mM indole and (B) 3 mM carbazole, each with 1 mM riboflavin (R) in $Me_2SO$-$d_6$. Diphenylamine, triphenylamine, dimethylaniline, *N*-ethylcarbazole, and indoline show the same pattern of polarization as carbazole (the polarization of the tertiary amines is much weaker than that of the secondary amines at comparable concentrations). Tetrahydrocarbazole shows the same pattern as indole.

amine proton and the protons ortho and para to the nitrogen (positions 1, 3, 6, 8, and 9 in carbazole) show substantial positive polarization, while the other positions show weak negative polarization. Indoline (2,3-dihydroindole) and diphenylamine show the same pattern, and all of these are the reverse of the pattern for the indoles.

Reliable calculations of the unpaired spin density distribution in open-shell, heterocyclic nonalternate systems are notoriously rare. Although there have been a number of much more advanced calculations of the electronic structure of the indole ground and excited states in the last few years, these studies have focused primarily on the assignment of electronic transitions, molecular geometry, and ionization potentials (Selsby & Grimison, 1977; Evleth et al., 1977; Mehlhorn et al., 1978). Given the absence of experimental data on the radical, it is not surprising that these calculations do not ad-

[3] For indole and 4-methylindole, polarization of the 1 proton is not seen. This may be due to faster exchange rates of these protons with traces of $H_2O$, which would remove the polarized proton, or to minor variations in the spin-density distribution. In 1-methylindole, the 1-methyl protons are polarized in emission.

dress spin densities. The INDO method tends to be more reliable than most approximate methods for the calculation of unpaired spin densities; however, it clearly fails for this ring system. A detailed examination of the eigenvalues and eigenvectors produced by the INDO calculations gives some indication of the origin of this failure. There are a number of near degenerate $\pi$ orbitals which have eigenvalues very close to that of the HOMO. These orbitals undoubtedly interact strongly, and a single determinant wave function does not properly represent such interaction. Use of configuration interaction (absent in INDO calculations) could alleviate this problem.

The INDO method generates corresponding orbitals for $\alpha$ and $\beta$ spins with very similar, though not exactly identical, coefficients. One would normally expect that the orbitals with very similar coefficients would have very similar energies, and thus that the coefficients of the $\alpha$ HOMO and $\beta$ LUMO would be very similar, as is the case in INDO calculations for alternate hydrocarbons such as anthracene. However, in the calculation for indole, the coefficients of the $\alpha$ and $\beta$ HOMOs are very similar, as are those of the $\beta$ LUMO and the next to the highest occupied $\alpha$ orbital. The presence of this orbital crossing raises the possibility that the INDO program has selected the wrong orbital as one of the HOMOs. This would have a profound effect on the induced spin densities in the lower occupied orbitals, changing the calculated spin densities and hyperfine coupling constants. A further indication of the problem with the INDO calculation is the extreme sensitivity of the spin densities to small geometrical variations. Use of Pople and Beveridge's recommended standard bond lengths or the bond lengths and angles taken from the tryptophan crystal structure (Takigawa et al., 1966), rather than those from the 3-methylindole crystal structure, changes the signs as well as the magnitudes of some of the calculated hyperfine coupling constants, whereas the CIDNP patterns of tryptophan and 3-methylindole are identical. Neither the total electronic energy nor the charge–density distribution is significantly affected by these geometry changes. Thus, the sensitivity of the calculated spin densities to geometry is probably a consequence of the lack of symmetry of the indole ring system, which imposes no nodal constraints on the wave functions.

The electronic wave functions in the INDO calculations are based on spin-unrestricted determinants of molecular orbitals, which are not in general eigenfunctions of $S^2$, and may contain contaminating contributions from states of higher multiplicity. The calculated spin densities which agree most closely with our experimental results are those of Evleth et al. (1973), who consider only $\pi$ electrons. Although this work employs quartet annihilation techniques, this is reported to have little affect on the resulting spin densities. Furthermore, the spin densities are quite sensitive to the value chosen for the C–N resonance integral. We believe that the modest agreement between this calculation and the CIDNP data is fortuitous, and we are presently attempting to resolve these discrepancies by using recently developed methods for open-shell molecules (Bacon & Zerner, 1979).

*Mechanistic Complications.* As discussed earlier, it is conceivable that the radical intermediate whose spin density determines the CIDNP polarization pattern is not the Trp radical cation. It is possible, for example, that some impurity reversibly attacks the initially formed cation radical at the 2 position:

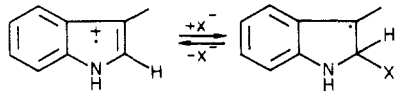

This radical would be comparable to a benzyl radical, with large spin densities expected at positions 3, 4, and 6 and nodes at positions 5 and 7. However, contrary to observation, the largest hyperfine interaction would be predicted for the proton at position 2 in this hypothetical intermediate as it lies above or below the plane of the radical. Furthermore, the sign of the hyperfine coupling constant would be opposite to that at position 3. We would also expect to detect polarization from the recombination product containing X, but polarization is only detected in the starting material. The polarization patterns for carbazole and indoline would be consistent with this explanation if their polarization patterns truly reflect the spin-density distributions in their respective radical cations, which cannot be attacked $\alpha$ to the nitrogen because of steric constraints in the former and the aliphatic ring in the latter. Substitution of a methyl at position 2 in Trp or indole has no effect on the polarization pattern, and tetrahydrocarbazole, which is as hindered as carbazole or indoline, behaves exactly like Trp. We detect the identical pattern for Trp in a very wide range of compounds and solvents, including proteins [see also Kaptein et al. (1978b)]. A similar analysis argues against attack at position 3.

Another concern is the tendency of Trp to form complexes with flavins (Tollin, 1968; McCormick, 1977). It is unlikely that this has an effect on the polarization pattern because the development of nuclear polarization requires freely diffusing, solvent-separated radical pairs for $S–T_0$ mixing. Consequently, the polarization pattern reflects the properties of the free radical, rather than a complex. Furthermore, we find that the flavin concentration does not alter the polarization pattern and that the pattern is independent of ring substitution, which might limit or alter complexation. Complexation is expected to affect the absolute polarization intensity, which should be remembered when assessing the relative intensities of Trp, His, and Tyr polarization in peptides and proteins. Finally, the same pattern is observed in the presence or absence of dissolved oxygen, which rules out attack by molecular oxygen. Given the bulk of chemical evidence, we favor the idea that the CIDNP intensities reflect the spin-density distribution in the radical cation and the mechanism in Scheme II.

*Gramicidin—An Example.* Gramicidin provides an example of the ability of high-resolution laser CIDNP of Trp to enhance the information content of NMR spectra. The gramicidins are linear pentadecapeptide antibiotics which have attracted a great deal of interest because they render biological membranes and synthetic lipid bilayers permeable to monovalent alkali cations and protons by forming transmembrane channels (Weinstein et al., 1979). The actual mode of antibiotic action has recently been shown to be related to the ability of the gramicidins to inhibit RNA synthesis (Paulus et al., 1979).

The sequence of valine-gramicidin A is

formyl-L-Val-Gly-L-Ala-D-Leu-L-Ala-D-Val-L-Val-D-Val-L-Trp-D-
1 2 3 4 5 6 7 8 9

Leu-L-Trp-D-Leu-L-Trp-D-Leu-L-Trp-NHCH$_2$CH$_2$OH
10 11 12 13 14 15

Gramicidin B has Trp-11 substituted by Phe, and gramicidin C has Trp-11 substituted by Tyr. The structure of the Trp-rich end of this polypeptide is intriguing, as the molecule is capable of forming helices, and it appears that the repeating D-Leu-L-Trp sequence is critical for interaction with RNA polymerase (Paulus et al., 1979).

The dark spectra and light minus dark spectra of gramicidins A and B are shown in Figure 8. All Trp residues in gramicidin A and B are polarized, and Tyr-11 in gramicidin

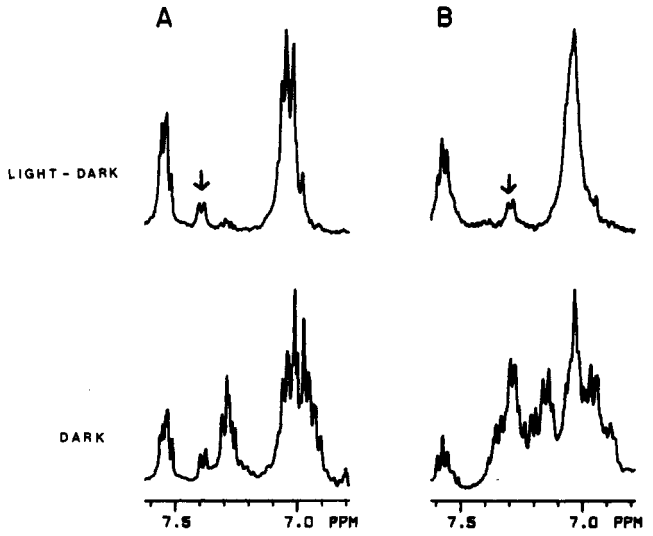


FIGURE 8: $^1$H NMR (360 MHz) dark spectra and light minus dark difference spectra of (A) 5 mM gramicidin A and (B) 3 mM gramicidin B, each in methanol-$d_4$ with 5 mM lumiflavin. The arrows indicate the single upfield-shifted Trp-4 proton.

C is also polarized (not shown). It is seen that the 4 proton in one of the Trp residues is shifted upfield considerably; this peak would be entirely obscured in the spectrum of gramicidin B by the Phe ring and Trp-7 protons. Since this upfield-shifted peak is observed in gramicidin C, it cannot be Trp-11. We believe that the upfield-shifted resonance is the result of single-stranded $\pi_6$ (L,D) helix formation in this solvent, consistent with studies by other workers. In models of this type of helix, Trp-15 and -9 are in close proximity; thus, the upfield shift may be caused by ring-current interactions between these residues. At this time, these spectra are presented primarily to illustrate another dimension which laser-induced photochemical reactions and CIDNP can bring to the NMR spectroscopy of complex peptides. A detailed study of gramicidin's interactions with itself, bilayers, and RNA polymerase by using the laser CIDNP method is in progress.

## Conclusions

In conclusion, we have shown that the reaction of photoexcited flavins with Trp is primarily an electron-transfer reaction, and the magnitude of the resulting CIDNP may depend critically on electron or hydrogen atom exchange rates. Since electron transfer is expected to be less regiospecific than hydrogen abstraction, the observation of CIDNP for Trp does not guarantee that the photoexcited dye makes direct contact with the residue. Of course, the absence of CIDNP from Trp or any other residue proves very little, because the CIDNP intensity is extremely sensitive to very minor structural perturbations, even in small peptides (E. F. McCord and S. G. Boxer, unpublished experiments). The spin-density distribution in the Trp radical cation has been determined and analyzed for the first time and correlates well with the reported chemical reactivity of the indole nucleus. Approximate molecular orbital calculations of the spin-density distribution are too sensitive to geometry and other parameters to be reliable for this unsymmetrical molecule, and we hope that the data will generate further theoretical interest. Because of the importance of this radical as an intermediate in the ultraviolet photolysis of biological materials, it will be very interesting to see if CIDNP can be detected during direct irradiation, thereby avoiding some of the complications with flavin photochemistry.

## Acknowledgments

We thank Dr. Woodrow Connover for assistance in the design of the probe used in these experiments and Professor John Brauman for helpful discussions on the INDO method.

## References

Ambrose, J. F., Carpenter, L. L., & Nelson, R. F. (1975) *J. Electrochem. Soc. 122*, 876–894.
Bacon, A. D., & Zerner, M. C. (1979) *Theor. Chim. Acta 53*, 21–54.
Ballard, S. G., Mauzerall, D. C., & Tollin, G. (1976) *J. Phys. Chem. 80*, 341–351.
Baudet, J., Berthier, G., & Pullman, B. (1962) *C. R. Hebd. Seances Acad. Sci. 254*, 762–764.
Boxer, S. G. (1976) Ph.D. Thesis, University of Chicago.
Boxer, S. G., & Closs, G. L. (1975) *J. Am. Chem. Soc. 97*, 3268–3270.
Casteleijn, G., Depireux, J., & Müller, A. (1964) *Int. J. Radiat. Biol. Relat. Stud. Phys., Chem. Med. 8*, 157–164.
Chambers, R. W., & Kearns, D. R. (1969) *Photochem. Photobiol. 10*, 215–219.
Closs, G. L., & Trifunac, A. D. (1970) *J. Am. Chem. Soc. 92*, 2183–2184.
Closs, G. L., & Czeropski, M. S. (1977) *Chem. Phys. Lett. 45*, 115–116.
Closs, G. L., & Czeropski, M. S. (1978) *Chem. Phys. Lett. 53*, 321–324.
Cohen, J. S. (1971) *Biochim. Biophys. Acta 229*, 603–609.
Dewar, M. J. S., & Trinajstic, N. (1971) *J. Chem. Soc. A*, 1220–1237.
Donovan, J. W. (1969) in *Physical Principles and Techniques of Protein Chemistry* (Leach, S. J., Ed.) Academic Press, New York.
Eriksson, L. E. G., & Ehrenberg, A. (1964) *Acta Chem. Scand. 18*, 1437–1453.
Evleth, E. M., Horowitz, P. M., & Lee, T. S. (1973) *J. Am. Chem. Soc. 95*, 7948–7955.
Evleth, E. M., Chalvet, O., & Bamlère, P. (1977) *J. Phys. Chem. 81*, 1913–1917.
Fleming, G. R., Morris, J. M., Robbins, R. J., Woolfe, G. J., Thistlethwaite, P. J., & Robinson, G. W. (1978) *Proc. Natl. Acad. Sci. U.S.A. 75*, 4652–4656.
Flossmann, W., & Westhof, E. (1978) *Radiat. Res. 73*, 75–85.
Forbes, W. F., & Sullivan, P. D. (1967) *Can. J. Biochem. 45*, 1831–1839.
Fukui, K., Yonezawa, T., Nagata, C., & Shingu, H. (1954) *J. Chem. Phys. 22*, 1433–1435.
Hanson, A. W. (1964) *Acta Crystallogr. 17*, 559–568.
Heelis, P. F., Parsons, B. J., Phillips, G. O., & McKellar, J. F. (1978) *Photochem. Photobiol. 28*, 169–173.
Kaptein, R. (1971) *J. Chem. Soc., Chem. Commun.*, 732–733.
Kaptein, R. (1978) in *Nuclear Magnetic Resonance Spectroscopy in Molecular Biology* (Pullman, B., Ed.) pp 211–229, Reidel, Dordrecht, The Netherlands.
Kaptein, R., Dijkstra, K., & Nicolay, K. (1978a) *Nature (London) 274*, 293–294.
Kaptein, R., Dijkstra, K., Müller, F., van Schagen, C. G., & Visser, A. J. W. G. (1978b) *J. Magn. Reson. 31*, 171–176.
Knibbe, H., Rehm, D., & Weller, A. (1968) *Ber. Bunsenges. Phys. Chem. 72*, 257–263.
Koch, T. R., & Purdy, W. C. (1972) *Talanta 19*, 989–1007.
Kreilick, R. W., & Weissman, S. I. (1966) *J. Am. Chem. Soc. 88*, 2645–2652.
Kurahashi, M., Fukuyo, M., Shimada, A., Furusaki, A., & Nitta, I. (1969) *Bull. Chem. Soc. Jpn. 42*, 2174–2179.
Lamola, A. A., Manion, M. L., Roth, H. D., & Tollin, G. (1975) *Proc. Natl. Acad. Sci. U.S.A. 72*, 3265–3269.
Lepley, A. R., & Closs, G. L., Eds. (1973) *Chemically Induced*

*Magnetic Polarization*, Wiley, New York.
Maki, A. H., & Zuchlich, J. A. (1975) *Top. Curr. Chem. 54*, 115-163.
McCormick, D. B. (1977) *Photochem. Photobiol. 26*, 169-182.
McDonald, G. G., & Leigh, J. S., Jr. (1973) *J. Magn. Reson. 9*, 358-362.
Mehlhorn, A., Schwenzer, B., Brückner, H. J., & Schwetlick, K. (1978) *Tetrahedron 34*, 481-486.
Momicchioli, F., & Rastelli, A. (1967) *J. Mol. Spectrosc. 22*, 310-324.
Moore, W. M., & Baylor, C., Jr. (1969) *J. Am. Chem. Soc. 91*, 7170-7179.
Müller, F., Hemmerich, P., Ehrenberg, A., Palmer, G., & Massey, V. (1970) *Eur. J. Biochem. 14*, 185-196.
Munro, I., Pecht, I., & Stryer, L. (1979) *Proc. Natl. Acad. Sci. U.S.A. 76*, 56-60.
Muus, L. T., Atkins, P. W., McLauchlan, K. A., & Pedersen, J. B., Eds. (1977) *Chemically Induced Magnetic Polarization*, Reidel, Dordrecht, The Netherlands.
Nicholson, R. S., & Shain, I. (1965) *Anal. Chem. 37*, 178-190.
Pailthorpe, M. T., & Nicholls, C. H. (1971) *Photochem. Photobiol. 14*, 135-145.
Paulus, H., Sarkar, N., Mukherjee, P. K., Langley, D., Ivanov, V. T., Shepel, E. N., & Veatch, W. (1979) *Biochemistry 18*, 4532-4541.
Penzer, G. R., & Radda, G. K. (1967) *Q. Rev., Chem. Soc. 21*, 43-65.
Pople, J. A., & Beveridge, D. L. (1970) *Approximate Molecular Orbital Theory*, McGraw-Hill, New York.
Potts, K. T., & Saxton, J. E. (1973) *Org. Synth., Coll. Vol. 5*, 769-770.
Redfield, A. G., & Kunz, S. D. (1979) in *NMR and Biochemistry* (Opella, S. J., & Lu, P., Eds.) pp 225-239, Marcel Dekker, New York.
Redfield, A. G., Kunz, S. D., & Ralph, E. K. (1975) *J. Magn. Reson. 19*, 114-117.
Ross, J. B. A., Rousslang, K. W., & Kwiram, A. L. (1980) *Biochemistry 19*, 876-883.
Rydon, H. N. (1948) *J. Chem. Soc.*, 705-710.
Saito, I., Matsuura, T., Nakagawa, M., & Hino, T. (1977) *Acc. Chem. Res. 10*, 346-352.
Sandros, K. (1964) *Acta Chem. Scand. 18*, 2355-2374.
Sawyer, D. T., & Roberts, J. L., Jr. (1974) *Experimental Electrochemistry for Chemists*, Wiley, New York.
Selsby, R. G., & Grimison, A. (1977) *Int. J. Quantum Chem. 12*, 527-544.
Stryer, L., & Haugland, R. P. (1967) *Proc. Natl. Acad. Sci. U.S.A. 58*, 719-726.
Sundberg, R. J. (1970) *The Chemistry of the Indoles*, p 78, Academic Press, New York.
Takigawa, T., Ashida, T., Sasada, Y., & Kakudo, M. (1966) *Bull. Chem. Soc. Jpn. 39*, 2369-2378.
Tatwawadi, S. V., Santhanam, K. S. V., & Bard, A. J. (1968) *J. Electroanal. Chem. Interfacial Electrochem. 17*, 411-420.
Tollin, G. (1968) *Molecular Associations in Biology* (Pullman, B., Ed.) pp 393-409, Academic Press, New York.
Weinstein, S., Wallace, B. A., Blout, E. R., Morrow, J. S., & Veatch, W. (1979) *Proc. Natl. Acad. Sci. U.S.A. 76*, 4230-4234.
Wessels, P. L., Feeney, J., Gregory, H., & Gormley, J. J. (1973) *J. Chem. Soc., Perkin Trans. 2*, 1691-1698.
Yamashita, M., & Kashiwagi, H. (1974) *J. Phys. Chem. 78*, 2006-2009.
Yguerabide, J., Epstein, H. F., & Stryer, L. (1970) *J. Mol. Biol. 51*, 573-590.
Yoshida, K. (1979) *J. Am. Chem. Soc. 101*, 2116-2121.

# Hexagonal Phases in Phospholipids with Saturated Chains: Phosphatidylethanolamines and Phosphatidic Acids†

Karl Harlos* and Hansjörg Eibl

ABSTRACT: The structure of phospholipids with saturated chains was investigated by differential scanning calorimetry and by X-ray diffraction. It is shown that both phosphatidylethanolamines and phosphatidic acids can exhibit a hexagonal phase at high temperature. The temperature of the transition to the hexagonal phase is dependent on chain length and sodium salt concentration. Increasing the chain length or the sodium salt concentration results in a decrease in the transition temperature. In addition to this transition at high temperature, a calorimetric transition at low temperature is detected in some phospholipids.

Phospholipid/water systems can be regarded as simple models for biological membranes. It has been demonstrated that phospholipids can form lamellar structures as well as adopt so-called hexagonal phases. As the lamellar phase is dominant in phospholipids, most previous studies have dealt with lamellar structures. Hexagonal phases have been reported mainly for phospholipids with unsaturated chains, for example, for dioleoylphosphatidylethanolamine (Cullis & de Kruijff, 1976; Van Dijck et al., 1976), for phosphatidylethanolamines from natural sources (Reiss-Husson, 1967; Rand et al., 1971; Cullis & de Kruijff, 1978), and for (egg) phosphatidylserine (Hope & Cullis, 1980). For negatively charged phospholipids, it has been shown that divalent cations can induce hexagonal phases (Deamer et al., 1970; Rand & Sengupta, 1972; Papahadjopoulos et al., 1976; Cullis et al., 1978; Harlos & Eibl, 1980a,b). This study deals with the appearance of hexagonal phases in phospholipids with saturated chains in the presence of monovalent cations.

In the present paper, the term "hexagonal phase" is used solely to indicate the appearance of small-angle diffraction lines in the ratio of $1:1/3^{1/2}:1/2$ and is not restricted to a particular

† From the Max-Planck-Institut für biophysikalische Chemie, 34 Göttingen-Nikolausberg, Federal Republic of Germany. *Received October 13, 1980.* This work was supported by the Deutsche Forschungsgemeinschaft through SFB 33.

0006-2960/81/0420-2888$01.25/0 